

[Home](#) [Search](#) [Collections](#) [Journals](#) [About](#) [Contact us](#) [My IOPscience](#)

Domain wall magnetoresistance in BiFeO₃ thin films measured by scanning probe microscopy

This content has been downloaded from IOPscience. Please scroll down to see the full text.

Download details:

IP Address: 146.203.151.55

This content was downloaded on 20/06/2017 at 15:04

Manuscript version: Accepted Manuscript

Domingo et al

To cite this article before publication: Domingo et al, 2017, J. Phys.: Condens. Matter, at press:

<https://doi.org/10.1088/1361-648X/aa7a24>

This Accepted Manuscript is: © 2017 IOP Publishing Ltd

During the embargo period (the 12 month period from the publication of the Version of Record of this article), the Accepted Manuscript is fully protected by copyright and cannot be reused or reposted elsewhere.

As the Version of Record of this article is going to be / has been published on a subscription basis, this Accepted Manuscript is available for reuse under a CC BY-NC-ND 3.0 licence after the 12 month embargo period.

After the embargo period, everyone is permitted to copy and redistribute this article for non-commercial purposes only, provided that they adhere to all the terms of the licence

<https://creativecommons.org/licences/by-nc-nd/3.0>

Although reasonable endeavours have been taken to obtain all necessary permissions from third parties to include their copyrighted content within this article, their full citation and copyright line may not be present in this Accepted Manuscript version. Before using any content from this article, please refer to the Version of Record on IOPscience once published for full citation and copyright details, as permission will likely be required. All third party content is fully copyright protected, unless specifically stated otherwise in the figure caption in the Version of Record.

When available, you can view the Version of Record for this article at:

<http://iopscience.iop.org/article/10.1088/1361-648X/aa7a24>

1
2
3
4
5
6
7
8
9
10
11
12
13
14
15
16
17
18
19
20
21
22
23
24
25
26
27
28
29
30
31
32
33
34
35
36
37
38
39
40
41
42
43
44
45
46
47
48
49
50
51
52
53
54
55
56
57
58
59
60

Domain wall magnetoresistance in BiFeO₃ thin films measured by scanning probe microscopy

N. Domingo,¹ S. Farokhipoor,² J. Santiso¹, B. Noheda,² G. Catalan^{1,3}

¹ ICN2 - Institut Català de Nanociència i Nanotecnologia, CSIC and The Barcelona Institute of Science and Technology (BIST), Campus UAB, Bellaterra, 08193 Barcelona

² Nanostructures of Functional Oxides, Zernike Institute for Advanced Materials, University of Groningen, Nijenborgh 4, 9747AG Groningen, The Netherlands

³ ICREA - Institutio Catalana de Recerca i Estudis Avançats, 08010 Barcelona

Abstract:

We measure the magnetotransport properties of individual 71° domain walls in multiferroic BiFeO₃ by means of conductive – atomic force microscopy (C-AFM) in the presence of magnetic fields up to one Tesla. The results suggest anisotropic magnetoresistance at room temperature, with the sign of the magnetoresistance depending on the relative orientation between the magnetic field and the domain wall plane. A consequence of this finding is that macroscopically averaged magnetoresistance measurements for domain wall bunches are likely to underestimate the magnetoresistance of each individual domain wall.

Introduction

The field of domain wall nanoelectronics[1] owes to Ekhard Salje many of its foundation stones, and in particular the realization that domain walls offer extremely thin and yet topologically-protected percolative paths for charge transport, with additional functionality enabled by their controllable positioning [2]. Experimentally, Aird and Salje were the first to report a different transport regime in these extended nanostructures when they discovered evidence for superconductivity inside the ferroelastic twin walls of sodium-doped WO_3 . [3]

Later, scanning probe investigation of transport properties in undoped multiferroics led to the first direct observation of enhanced conductivity on artificially written DW's in thin films of BiFeO_3 (BFO) by Seidel et al., [4] while Chiu et al. [5] showed that enhanced conductivity existed not only in artificially written DW's but also in the walls of spontaneous epitaxially-induced twins. Farokhipoor and Noheda [6] reported the same finding and showed, in addition, that the magnitude of the current does not significantly depend on the type of ferroelastic domain walls (109° or 71° types) and that the conduction level is determined by the defect content. [7]

Even though different conduction mechanisms have been put forward by different works [5],[6],[8] enhanced conductivity appears in fact to be a fairly common effect not limited to multiferroic BFO; enhanced DW conductivity has also been reported in thin films of $\text{Pb}(\text{Zr},\text{Ti})\text{O}_3$ [9], or BaTiO_3 [10]; in improper ferroelectric single crystals of ErMnO_3 [11] and HoMnO_3 [12]; as well as in single crystals of LiNbO_3 . [13]

The influence of magnetic field on the transport properties of domain walls of BFO has also been studied, not by direct local-probe techniques, but by spatially-extended measurements where large electrodes connect arrays of DW's. The first report, by He et

1
2
3 al.,[14] demonstrated a significant magnetoresistance assigned to 109° ferroelectric DW's at
4
5 temperatures below 200 K and under fields of up to 7 T. The magnetoresistance exhibited
6
7 anisotropy as a function of the direction of the applied magnetic field, being negative when
8
9 both magnetic field and transport are parallel to the DW's, and zero otherwise. More recently,
10
11 Lee et al.,[15] also reported anisotropic magnetoresistance (AMR) on lithium-doped BFO
12
13 films at low temperatures. They performed the measurements in capacitor-like structures and
14
15 observed a unidirectional anisotropy accompanied by hysteresis. The peak in
16
17 magnetoresistance coincided with the peak in displacement current during ferroelectric
18
19 switching, consistent with magnetoresistance arising from domain walls, whose concentration
20
21 is indeed biggest half way through the switching process. On the other hand, since all
22
23 evidence to date is based on macroscopically averaged measurements, there is no indication
24
25 of how (or whether) each individual domain wall, with its own particular orientation with
26
27 respect to the external field, contributes differently to the total measured MR.
28
29
30
31
32
33
34

35 In this work we report the first attempt to directly measure the magnetoresistance at
36
37 room temperature of individual ferroelastic 71° BFO DW's, using conductive - atomic force
38
39 microscopy (C-AFM) under the presence of external applied magnetic fields up to one Tesla.
40
41 The 71° DW's of BFO were found to display an anisotropic MR and, importantly, the sign of
42
43 the MR in these walls appears to be positive or negative depending on the relative orientation
44
45 between field and wall. This is in contrast with the MR of 109° domain walls which is always
46
47 negative or zero.[14] While the generality of these results needs to be tested in different
48
49 samples and geometries; if confirmed, these results would imply that macroscopically
50
51 averaged measurements can underestimate the magnitude of the local MR at domain walls,
52
53 and that optimization of device response must therefore include engineering of the DW's so
54
55 that they are all of the same type and aligned in the same direction with respect to the external
56
57 magnetic field.
58
59
60

Methods

For this study, an epitaxial BFO thin film on SrRuO₃ (SRO)-covered DyScO₃ (001) single-crystal substrates have been prepared by pulsed laser deposition (PLD). The BFO film was 50nm thick and the SRO bottom electrode 6nm. The (110)_o-oriented DyScO₃ single-crystal substrate was singly terminated ScO₂. The single termination of the substrate was achieved by thermally treating the substrate at 900°C for 4 hours under 300 cc/min oxygen pressure.[16] This produces a surface with atomically flat vicinal terraces of c.a. 200nm width.

The base growth pressure of our PLD system is 10⁻⁷ mbar. The growth pressure and temperature are 0.3 mbar O₂ and 670°C, respectively. A pulsed KrF excimer laser (wavelength of 248 nm) with a repetition rate of 0.5 Hz and energy density of 2 J/cm² was focused on the BFO target for 4 hours during the thin film growth. After deposition, the sample were annealed at 120 mbar oxygen ambient pressure with a cooling rate of 3°C/min. The films are grown atomic-layer-by-atomic-layer, as observed by in-situ RHEED oscillations, and are atomically flat, following the also atomically flat terraces of the DyScO₃ substrate, as confirmed by AFM topographic measurements (Figure 1-b). The epitaxy and crystallography was examined by x-ray diffraction (XRD) using a Bruker x-ray 4-circle diffractometer (Figures 1-c and 1-d).

The ferroelectric configuration was probed by piezoresponse force microscopy (PFM) on an Asylum MFP3D in DART mode, by exciting the sample with a V_{ac} voltage applied to the sample at two different frequencies around the contact resonance frequency. Vertical and horizontal cantilever oscillation modes were used to characterize the orientation of the ferroelectric polarization, allowing to map the ferroelectric domain configuration, which consists of 71 degree domains as sketched in Figure 1-a.

1
2
3 The magnetotransport measurements at room temperature were done by C-AFM in
4 the presence of an in-plane magnetic field applied in-situ at the same Asylum equipment. The
5 current was measured using an ORCA tip holder with a current amplifier of $5 \cdot 10^9$ placed next
6 to the grounded tip in combination with the Asylum's VFM-2 sample holder, which uses a
7 permanent magnet placed under the sample that can be rotated within a horseshoe-shaped
8 metallic structure to vary the in-plane magnetic field between 0 and 1 T at the sample
9 position. For these measurements, mMasch NSC18 Pt tip were used, with conductive non-
10 magnetic Pt coating.
11
12
13
14
15
16
17
18
19
20
21
22

23 After each measurement, PFM images were taken on the same area to confirm the
24 stability of the DW and the absence of possible dynamic DW effects on the transport
25 measurements. The applied voltage was kept limited to < 2 V (voltage applied to the bottom
26 electrode) in order to avoid switching of the polarization, which would yield spurious
27 displacement currents rather than true transport. Here it is worth noticing that although such
28 events could also be avoided altogether by applying negative instead of positive voltages,
29 there is a strong diode-like response of the domain walls, which show no appreciable current
30 transport for negative biases.[6]
31
32
33
34
35
36
37
38
39
40
41
42
43
44
45

46 **Results**

47
48
49 X-Ray diffraction patterns confirm the fully coherent and epitaxial growth of the film
50 with respect to the substrate (figures 1-c and 1-d). The off-specular reciprocal space map
51 around the pseudocubic (103) reflection (figure 1-d) show that the film has the same in-plane
52 lattice parameter and peak width as the substrate. Additionally, the film's peak-splitting
53 shows the existence of ferroelastic domains, corresponding to the monoclinic r3 and r4
54 variants as defined by Chen *et al.*[17]
55
56
57
58
59
60

1
2
3 Because of the electrostatic boundary condition (bottom electrode and exposed top
4 surface), there is a built-in field that favors downward polarization (see figure 2-b) and thus
5 only 4 out of the 8 possible polarization orientations (figure 2-c). Therefore, only two types
6 of domain walls can be present: those that separate polarization directions that differ by 109°
7 and those that separate polarization directions that differ by 71° . However, as characterized
8 by PFM, the great majority of domain walls are 71° DW parallel to the $\langle 100 \rangle$ or $\langle 010 \rangle$
9 directions. Vector PFM images (VPFM) in Figure 2 show the distribution of domains with
10 alternating in-plane polarization, and uniform out of plane polarization.[18] The domains are
11 of a fairly uniform width around 120 ± 10 nm.
12
13
14
15
16
17
18
19
20
21
22
23
24

25 C-AFM was used to study the conductive properties of the DW following the sketch
26 shown in Figure 3. The Pt-coated AFM tip was used as a top mobile electrode. The C-AFM
27 image on the same area shown in Figure 2 shows a pattern of straight lines fully consistent
28 with the presence of the DW as observed by VPFM, giving evidence of the enhanced
29 conductivity of the domain walls. Single point C-AFM measurements allow obtaining of $I(V)$
30 curves at different locations of the sample, with a lateral resolution of the order of few
31 nanometers.
32
33
34
35
36
37
38
39
40
41
42

43 To analyse the magnetic-field dependence of the observed conductivity, in-plane
44 magnetic fields of up to 1 T were applied parallel to the thin film plane in the (100) direction
45 while measuring $I(V)$ curves at different spots on the DW's. In order to account for the
46 anisotropy of magnetoresistance effects, two different families of DW placed parallel and
47 perpendicular to the applied magnetic field were analysed. When the magnetic field is
48 parallel to the in-plane orientation of the DW, it is also fully perpendicular to the transport
49 path (DW1, $H \perp I$). In contrast, when the magnetic field is perpendicular to the in-plane
50 direction of the domain wall (DW2), the current transport path is inclined at 45 degrees with
51
52
53
54
55
56
57
58
59
60

1
2
3 respect to the magnetic field (given the ~ 45 degree angle that this type of domain walls forms
4 with the substrate) and, therefore, it includes two components: one with the field
5 perpendicular both to the current direction ($H \perp I$) and the plane of the domain wall, and one
6 with the field parallel to the current ($H // I$, see sketch in Figure 3).
7
8
9
10
11

12
13
14 I(V) curves were measured at different points on the sample, discarding any
15 measurements where local ferroelectric switching (and thus ferroelectric displacement
16 currents) had been induced by the external voltage. Over twenty such conductivity
17 measurements with and without magnetic field were registered and compared; despite small
18 quantitative differences between measurements, the qualitative behaviour was always the
19 same, and representative examples of each type shown in Figure 4.
20
21
22
23
24
25
26
27
28

29 The results show two qualitatively different magnetoresistive responses: for the family
30 of DW1 (field parallel to the in-plane direction of the wall), the magnetic field does not have
31 a strong effect on transport, and appears to only slightly increase the conductivity, consistent
32 with a small negative magnetoresistance as reported also for 109° domain walls.[19]. In
33 contrast, for the family of DW2, the magnetic field decreases the conductivity.
34
35
36
37
38
39
40
41
42
43
44

45 Discussion

46
47
48 It is noteworthy that the magnitude of the magnetoresistance at room temperature is
49 larger than observed in macroscopically averaged measurements such as those of Lee *et*
50 *al.*[15] The discrepancy is consistent with the observed magnetoresistive anisotropy: if walls
51 with different orientation with respect to the magnetic field yield MR of different signs, their
52 contributions can mutually cancel in macroscopically averaged measurements. An important
53
54
55
56
57
58
59
60

1
2
3
4
5
6
7
8
9
10
11
12
13
14
15
16
17
18
19
20
21
22
23
24
25
26
27
28
29
30
31
32
33
34
35
36
37
38
39
40
41
42
43
44
45
46
47
48
49
50
51
52
53
54
55
56
57
58
59
60

lesson is therefore that macroscopically-averaged measurements can underestimate the local magnetoresistance of individual domain walls.

The other important result is of course the observation that magnetoresistance is anisotropic. This observation poses questions about the origin of the observed MR, and the cause of its anisotropy. Presently, we can only speculate: spin disorder in magnetic semiconductors is known to increase their resistivity and, conversely, magnetic fields increase spin alignment and thus cause negative magnetoresistance [20]. In some mixed valence perovskites, such as manganites, large negative magnetoresistance can also be induced by double-exchange [21, 22]. Either explanation requires a non-homogeneous ground state and would be consistent with an increased oxygen vacancy concentration at the domain wall (oxygen vacancies at the wall that change the local oxidation state of the Fe and its magnetic configuration), which in turn is also consistent with their conductivity mechanism [7].

In contrast, the positive MR for DW2, may be explained by a different mechanism that does not even require the domain walls to be magnetic to start with. Specifically, so-called geometric magnetoresistance is to be expected in a configuration with a magnetic field partially perpendicular to a transport plane. Such geometry induces a Lorentz force on the carriers that deviates their transport path, resulting in positive magnetoresistance.[23] This effect happens even in classic semiconductors such as silicon,[24] and is strongest in disordered systems.[25] Thus, while having fundamentally different origins, both negative and positive magnetoresistance can benefit from defect-induced disorder at the domain walls.

Of course, although our measurements are statistically robust and repeatable within our sample, it would be adventurous to assert the generality of the observed behaviour for other samples –particularly if, as discussed, it is likely to be influenced by defects. Extending

1
2
3 these studies to different types of ferroelectric walls (109 degree, 180 degree) on films grown
4 on different substrates and under different oxygen annealing conditions would be a helpful
5
6 next step in that regard. Generally, however, domain walls are known to attract and be
7
8 attracted to defects such as oxygen vacancies, and, in our case, the presence of such defects is
9
10 consistent with the observed inhomogeneity in the domain wall current, as evidenced by
11
12 alternating hotspots and darker regions in the conductivity profiles of the walls (Figure 3-c).
13
14
15 Domain walls are also, due to their geometry, good candidates to display geometry-driven
16
17 positive MR behaviour.
18
19
20
21
22

23 The two main lessons from this discussion are that (i) defects are likely to increase
24
25 DW magnetoresistance (both positive and negative) by introducing disorder at the wall and
26
27 (ii) since geometric magnetoresistance does not require the semiconducting material to be
28
29 magnetic, it is possible that all ferroelectric domain walls, and not just those of BiFeO_3 , be
30
31 prone to MR effects. This latter hypothesis, however, remains to be tested.
32
33
34
35
36
37

38 **Acknowledgements**

39
40 GC., N.D and J. S. acknowledge funding from MINECO grant MAT2016-77100-C2-1-P and
41
42 Generalitat de Catalunya grant 2014-SGR-1216. ND also acknowledges funding from
43
44 “Ramon y Cajal” contract RYC-2010-06365 and FIS2015-73932-JIN from MINECO. ICN2
45
46 acknowledges support of the Spanish MINECO through the Severo Ochoa Centers of
47
48 Excellence Program under Grant SEV-2013-0295.
49
50
51
52
53
54
55
56
57
58
59
60

Figure 1:

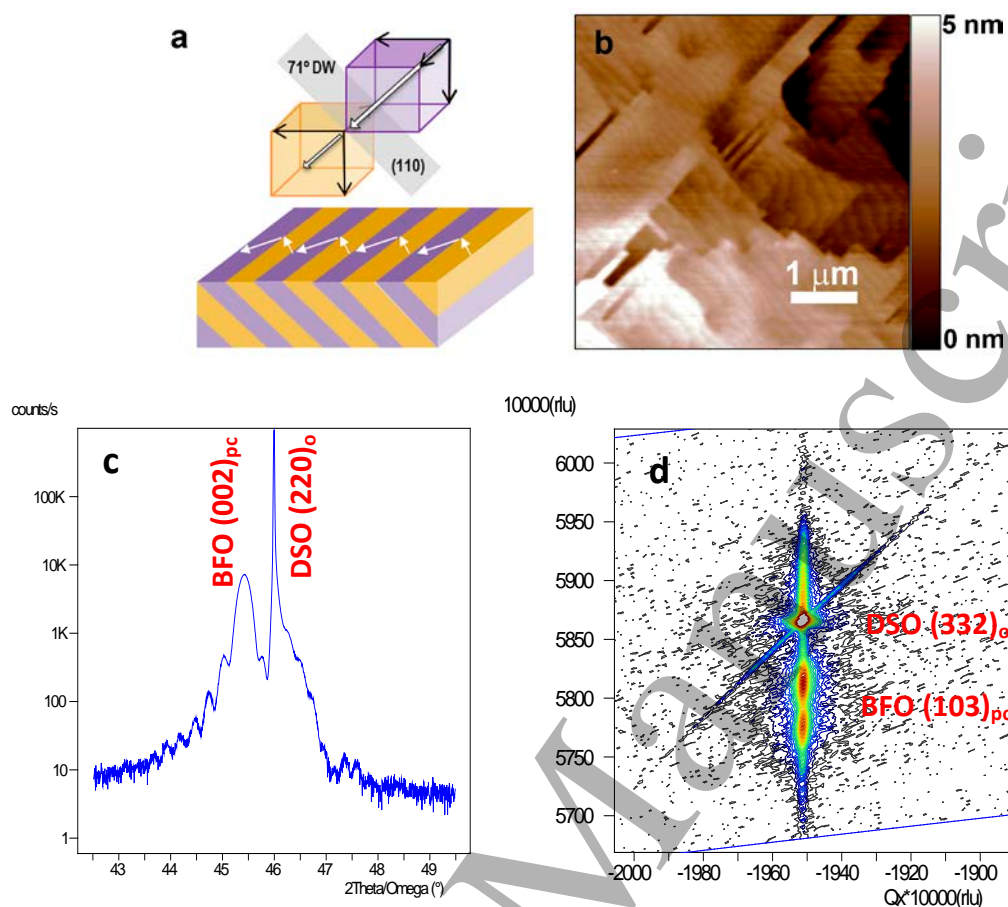


Figure 1. **a**, Configuration of as grown 71° ferroelectric DW's in BFO thin films, as characterized by PFM (see also Figure 2). **b**, Topography image obtained by AFM, showing atomically flat surfaces with unit-cell-high and 200-nm-wide vicinal steps. **c**, High resolution θ - 2θ X-ray diffraction scan around the 002 diffraction peak, showing good crystallinity and interfacial sharpness, as indicated by the satellite peaks (oscillation fringes) around the film's diffraction peak. **d**, Off-specular reciprocal space map around the BiFeO_3 $(103)_{\text{pseudocubic}}$ diffraction peak and the DyScO_3 $(332)_{\text{orthorhombic}}$ diffraction peak. Notice that the in-plane lattice parameter and peak width of the film coincides with that of the substrate, indicating coherent epitaxial growth. The BFO peak-split in the out-of-plane direction corresponds to the two angular variants of the ferroelastic 71° domains.

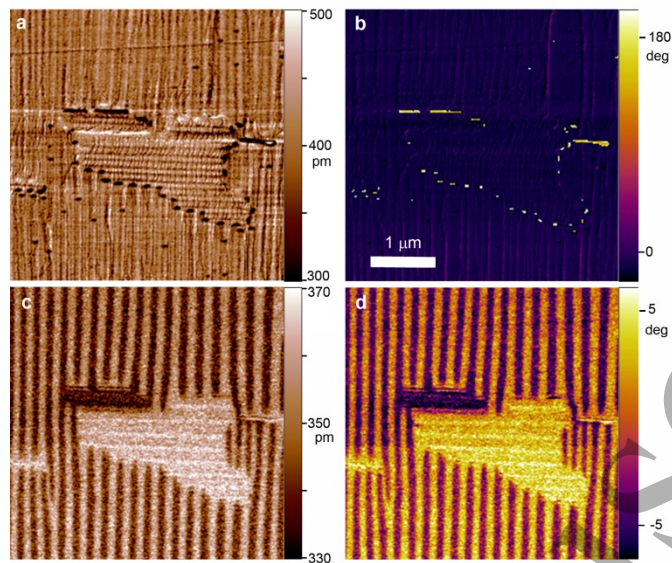
Figure 2:

Figure 2. Vector PFM mapping: **a**, Vertical PFM amplitude and **b**, PFM phase. **c**, Lateral PFM amplitude and **d**, PFM phase. Together, the results indicate that all the domains have the same downward out-of-plane polarization, with the polarity alternating only in the in-plane direction, consistent with 71 degree domains. The domain width is $120 \pm 10 \text{ nm}$.

Figure 3:

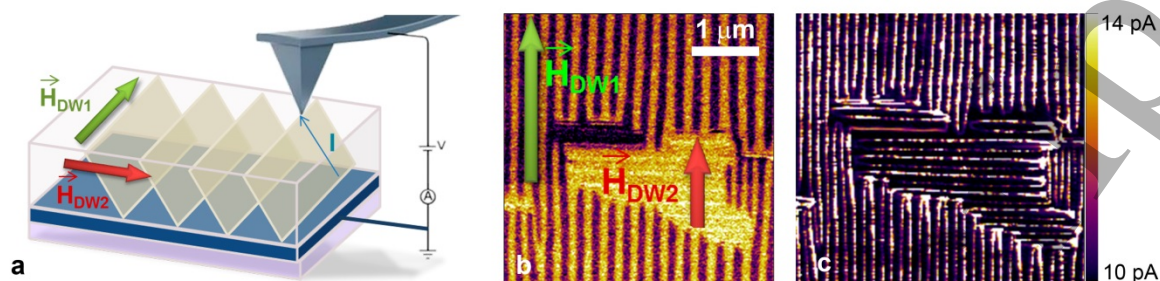


Figure 3. **a**, Scheme of the C-AFM configuration used for the magnetotransport measurements; it shows the relative orientations of the 71° DWs (shown in grey) with respect to the magnetic field in the two possible in plane directions (red and green arrows), and the transport path I between the tip and the substrate, shown as a blue vector lying within the plane of the DW. **b**, Lateral PFM phase image showing the two families of DWs used for the magnetoresistive measurements as described in the text, with different relative orientation of the magnetic field with respect to the DW, as sketched in **a** (note that from the experimental point of view, the direction of the in plane magnetic field is fixed and cannot be rotated). **c**, Current map measured with C-AFM prior to the application of any magnetic field. Notice that, while all the DW's are clearly conductive, the conduction is not homogeneous, as the lines show brighter "hotspots" of more intense current alternating with darker regions of weaker transport. This suggests that the conductivity is related to the presence of local defects at the walls.

Figure 4:

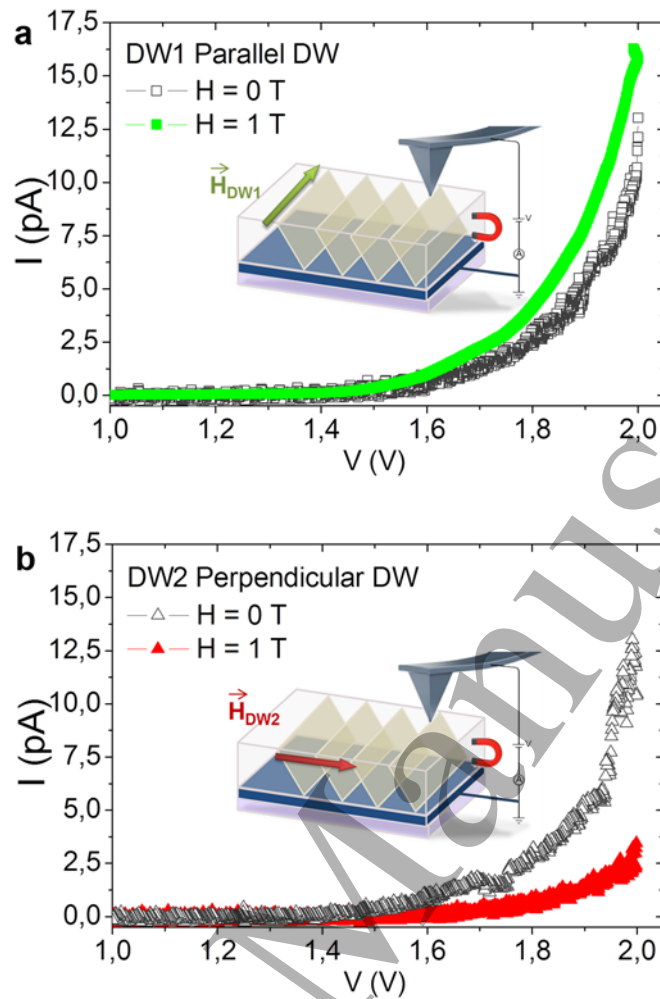


Figure 4. $I(V)$ curves obtained for DW1 and DW2, without and with the presence of a magnetic field, with a grounded tip while applying the voltage to the sample. It is observed that the current levels are independent of the DW orientation since both curves overlap, but the presence of a magnetic field of 1T leads to behaviour coherent to AMR. The enhancement of conductivity levels with the presence of a magnetic field for the families of DW1 is also in agreement with the appearance of some degree of ferromagnetic order at the DW along the transport path, while the decrease of conductivity for the family of domains of DW2 can be correlated with a charge concentration at both sides of the DWs due to Hall effect.

- 1
2
3
4 [1] G. Catalan, J. Seidel, R. Ramesh, J.F. Scott, Domain wall nanoelectronics, *Reviews of Modern Physics*, **84** (2012) 119-156.
- 5
6 [2] E.K.H. Salje, Multiferroic Domain Boundaries as Active Memory Devices: Trajectories Towards
7 Domain Boundary Engineering, *ChemPhysChem*, **11** (2010) 940-950.
- 8 [3] A. Aird, E. K. H. Salje, Sheet superconductivity in twin walls: experimental evidence of WO_{3-x} ,
9 *Journal of Physics: Condensed Matter*, **10** (1998) L377.
- 10 [4] J. Seidel, L.W. Martin, Q. He, Q. Zhan, Y.H. Chu, A. Rother, M.E. Hawkrigde, P. Maksymovych, P.
11 Yu, M. Gajek, N. Balke, S.V. Kalinin, S. Gemming, F. Wang, G. Catalan, J.F. Scott, N.A. Spaldin, J.
12 Orenstein, R. Ramesh, Conduction at domain walls in oxide multiferroics, *Nat Mater*, **8** (2009) 229-
13 234.
- 14 [5] Y.-P. Chiu, Y.-T. Chen, B.-C. Huang, M.-C. Shih, J.-C. Yang, Q. He, C.-W. Liang, J. Seidel, Y.-C. Chen,
15 R. Ramesh, Y.-H. Chu, Atomic-Scale Evolution of Local Electronic Structure Across Multiferroic
16 Domain Walls, *Advanced Materials*, **23** (2011) 1530-1534.
- 17 [6] S. Farokhipoor, B. Noheda, Conduction through 71° Domain Walls in BiFeO_3 Thin Films, *Physical*
18 *Review Letters*, **107** (2011) 127601.
- 19 [7] S. Farokhipoor, B. Noheda, Local conductivity and the role of vacancies around twin walls of
20 $(001)\text{-BiFeO}_3$ thin films, *Journal of Applied Physics*, **112** (2012) 052003.
- 21 [8] J. Seidel, P. Maksymovych, Y. Batra, A. Katan, S.Y. Yang, Q. He, A.P. Baddorf, S.V. Kalinin, C.H.
22 Yang, J.C. Yang, Y.H. Chu, E.K.H. Salje, H. Wormeester, M. Salmeron, R. Ramesh, Domain Wall
23 Conductivity in La-Doped BiFeO_3 , *Physical Review Letters*, **105** (2010) 197603.
- 24 [9] J. Guyonnet, I. Gaponenko, S. Gariglio, P. Paruch, Conduction at Domain Walls in Insulating
25 $\text{Pb}(\text{Zr}_{0.2}\text{Ti}_{0.8})\text{O}_3$ Thin Films, *Advanced Materials*, **23** (2011) 5377-5382.
- 26 [10] X.-K. Wei, A.K. Tagantsev, A. Kvasov, K. Roleder, C.-L. Jia, N. Setter, Ferroelectric translational
27 antiphase boundaries in nonpolar materials, *Nat Commun*, **5** (2014).
- 28 [11] D. Meier, J. Seidel, A. Cano, K. Delaney, Y. Kumagai, M. Mostovoy, N.A. Spaldin, R. Ramesh, M.
29 Fiebig, Anisotropic conductance at improper ferroelectric domain walls, *Nat Mater*, **11** (2012) 284-
30 288.
- 31 [12] W. Wu, Y. Horibe, N. Lee, S.W. Cheong, J.R. Guest, Conduction of Topologically Protected
32 Charged Ferroelectric Domain Walls, *Physical Review Letters*, **108** (2012) 077203.
- 33 [13] M. Schröder, A. Haußmann, A. Thiessen, E. Soergel, T. Woike, L.M. Eng, Conducting Domain
34 Walls in Lithium Niobate Single Crystals, *Advanced Functional Materials*, **22** (2012) 3936-3944.
- 35 [14] Q. He, C.H. Yeh, J.C. Yang, G. Singh-Bhalla, C.W. Liang, P.W. Chiu, G. Catalan, L.W. Martin, Y.H.
36 Chu, J.F. Scott, R. Ramesh, Magnetotransport at Domain Walls in BiFeO_3 , *Physical Review Letters*, **108**
37 (2012) 067203.
- 38 [15] J.H. Lee, I. Fina, X. Marti, Y.H. Kim, D. Hesse, M. Alexe, Spintronic Functionality of BiFeO_3
39 Domain Walls, *Advanced Materials*, **26** (2014) 7078-7082.
- 40 [16] J.E. Kleibeuker, B. Kuiper, S. Harkema, D.H.A. Blank, G. Koster, G. Rijnders, P. Tinnemans, E.
41 Vlieg, P.B. Rossen, W. Siemons, G. Portale, J. Ravichandran, J.M. Szeplieniec, R. Ramesh, Structure of
42 singly terminated polar DyScO_3 (110) surfaces, *Physical Review B*, **85** (2012) 165413.
- 43 [17] Z.H. Chen, A.R. Damodaran, R. Xu, S. Lee, L.W. Martin, Effect of "symmetry mismatch" on the
44 domain structure of rhombohedral BiFeO_3 thin films, *Applied Physics Letters*, **104** (2014) 182908.
- 45 [18] Y.H. Chu, Q. Zhan, L.W. Martin, M.P. Cruz, P.L. Yang, G.W. Pabst, F. Zavaliche, S.Y. Yang, J.X.
46 Zhang, L.Q. Chen, D.G. Schlom, I.N. Lin, T.B. Wu, R. Ramesh, Nanoscale Domain Control in
47 Multiferroic BiFeO_3 Thin Films, *Advanced Materials*, **18** (2006) 2307-2311.
- 48 [19] J. Feng, X. Qian, C.-W. Huang, J. Li, Strain-engineered artificial atom as a broad-spectrum solar
49 energy funnel, *Nature Photonics*, **6** (2012) 866-872.
- 50 [20] C. Haas, Spin-Disorder Scattering and Magnetoresistance of Magnetic Semiconductors, *Physical*
51 *Review*, **168** (1968) 531-538.
- 52 [21] C. Zener, Interaction between the d-Shell in the Transition Metals. II. Ferromagnetic
53 Compounds of Manganese with Perovskite Structure, *Physical Review*, **82** (1951) 403-405.
- 54
55
56
57
58
59
60

1
2
3 [22] P.G. de Gennes, Effects of Double Exchange in Magnetic Crystals, *Physical Review*, **118** (1960)
4 141-154.

5 [23] N.W. Ashcroft, N.D. Mermin, *Solid State Physics*, WILEY-VCH Verlag, New York, 1976.

6 [24] M.P. Delmo, S. Yamamoto, S. Kasai, T. Ono, K. Kobayashi, Large positive magnetoresistive effect
7 in silicon induced by the space-charge effect, *Nature*, **457** (2009) 1112-1115.

8 [25] M.M. Parish, P.B. Littlewood, Non-saturating magnetoresistance in heavily disordered
9 semiconductors, *Nature*, **426** (2003) 162-165.
10
11
12
13
14
15
16
17
18
19
20
21
22
23
24
25
26
27
28
29
30
31
32
33
34
35
36
37
38
39
40
41
42
43
44
45
46
47
48
49
50
51
52
53
54
55
56
57
58
59
60

Accepted Manuscript